

# Autocalibration with the Minimum Number of Cameras with Known Pixel Shape

José I. Ronda · Antonio Valdés · Guillermo Gallego

Received: date / Accepted: date

**Abstract** We address the problem of the Euclidean upgrading of a projective calibration of a minimal set of cameras with known pixel shape and otherwise arbitrarily varying intrinsic and extrinsic parameters. To this purpose, we introduce as our basic geometric tool the six-line conic variety (SLCV), consisting in the set of planes intersecting six given lines of 3D space in points of a conic. We show that the set of solutions of the Euclidean upgrading problem for three cameras with known pixel shape can be parameterized in a computationally efficient way. As a consequence, we propose an algorithm that performs a Euclidean upgrading with 5 (theoretical minimum) or more cameras with the knowledge of the pixel shape as the only constraint. We provide experiments with real images showing the good performance of the technique.

**Keywords** Camera autocalibration · Varying parameters · Square pixels · Three-dimensional reconstruction · Absolute Conic · Six Line Conic Variety

## 1 Introduction

Three-dimensional reconstructions from images are often obtained with calibrated cameras, i.e., cameras whose parameters have been previously computed using calibration objects in a controlled environment [10, p.201]. Unfortunately, in many cases such conditions are not available, e.g., when the images have been acquired with non-specialized

equipment or taken with a different initial purpose. To obtain 3D reconstructions without *a priori* knowledge of the camera parameters or the scene content, we need autocalibration algorithms, which allow for free variation of the camera parameters and provide a significant amount of flexibility in a wide variety of scenarios: we recall that just zooming a camera varies not only the focal length but also the location of the principal point [19].

The seminal paper [11] proposed the first autocalibration method, requiring images to be taken with cameras with constant intrinsic parameters. A common framework for autocalibration was later provided by the concept of geometric stratification [9,4]. This technique splits the camera calibration and scene reconstruction into three steps: first, the recovering of a projective reconstruction, i.e., a 3D scene and a set of cameras differing from the actual ones in a spatial homography. Second, an affine reconstruction, i.e., a reconstruction differing from the actual 3D scene in an affine transformation, is obtained by finding the location of the plane at infinity [12]. Finally, a Euclidean reconstruction, differing from the actual scene in a similarity, is found through the location of the absolute conic at infinity or any equivalent geometric object. A general reference for the subject is [6], where an extensive bibliography can be found.

In order to upgrade a projective reconstruction to an affine or a Euclidean one in the absence of knowledge about the scene, some data about the camera parameters must be available. For example, in the originally addressed autocalibration problem, this additional piece of data was the constancy of the camera intrinsic parameters [11], resulting, for each camera pair, in a couple of second-degree equations in the camera parameters known as Kruppa equations. The instability problems of these equations have been studied in [18].

Another constraint that has been studied is that in which the principal point is assumed to be known. Then the dual

---

José I. Ronda, Guillermo Gallego  
Grupo de Tratamiento de Imágenes, Universidad Politécnica de Madrid, 28040 Madrid, Spain  
E-mail: {jir,ggg}@gti.ssr.upm.es

Antonio Valdés  
Dep. de Geometría y Topología, Universidad Complutense de Madrid, 28040 Madrid, Spain  
E-mail: Antonio\_Valdes@mat.ucm.es

	AQC	SLCV
<i>Common features</i>		
Basic geometric object	Isotropic lines through the optical centers of the cameras	
Intrinsic parameter assumption	Known pixel shape (skew and aspect ratio)	
<i>Differences</i>		
Type of algorithm	Linear (solution of a homogeneous system)	Non-linear (bidimensional search using second degree equations)
Required number of cameras	$\geq 10$	$\geq 5$
Optimal w.r.t. number of cameras	No	Yes
Geometric object used	Quadric of $\mathbb{P}^5$	Algebraic surface of $\mathbb{P}^{3*}$
Degree of the geometric object	2	5
Geometrical meaning	Lines intersecting the absolute conic	Planes with conics intersecting all the isotropic lines
Integration with scene knowledge	Pairs of orthogonal lines	Parallel lines. Points at infinity

**Table 1** Comparison of the Absolute Quadratic Complex (AQC) and the Six-Line Conic Variety (SLCV) approaches.

absolute quadric [21] can be found by solving a set of homogeneous linear equations [16].

In this paper we address the problem of autocalibration in its less restrictive setting in practice: cameras with arbitrarily varying parameters with the exception of the pixel shape, which is assumed to be known. It can be easily seen (see section 2) that this is equivalent to having cameras with square pixels. The possibility of employing this constraint was studied in [7], where an algorithm based on bundle adjustment was considered. Algorithms based on this restriction have also been proposed [13, 22, 23] that result in a set of linear equations, but with the drawback of requiring 10 or more cameras. These algorithms are inspired by the geometric observation that, from the optical center of each square-pixel camera, two lines can be identified in the projective reconstruction that must intersect the absolute conic. The absolute quadratic complex (AQC) encodes the set of lines intersecting this conic by means of a quadric in  $\mathbb{P}^5$ , which is the natural space containing Plücker coordinates of lines. The AQC, being represented by a homogeneous symmetric  $6 \times 6$  matrix satisfying a linear constraint, depends linearly on  $21 - 1 - 1 = 19$  non-homogeneous parameters, which explains the need for such a high number of 10 views.

However, an informal parameter count reveals that far fewer cameras are theoretically sufficient. In fact, our main unknown is a space homography, which depends on 15 parameters. Being our target reconstruction defined up to a similarity, which depends on 7 parameters, there are  $15 - 7 = 8$  unknowns left to be found, which correspond to the degrees of freedom (dof) needed to determine the plane at infinity (3 dof) and the absolute conic within it (5 dof). Knowing camera skew and aspect ratio amounts to two equations per camera and thus at least 4 cameras should be given in order to solve the problem. Given the non-linear nature of these equations, multiple solutions can be expected and so 5 cameras should be the minimum required to obtain, generically, a unique solution (see [6, Table 19.3]).

The main goal of this paper is to obtain a Euclidean reconstruction from the minimum number of cameras using

exclusively the pixel shape restriction. The geometric object that will be employed for this purpose is the variety of conics intersecting six given spatial lines simultaneously, which will be termed the six-lines conic variety (SLCV). The SLCV as a geometrical entity has been studied in [15], although our treatment is independent and self-contained. In this paper we are interested in the SLCV given by the absolute conic at infinity.

The SLCV for six lines in generic position can be identified with a surface of  $\mathbb{P}^{3*}$  (i.e., the projective space given by the planes of  $\mathbb{P}^3$ ) of degree 8. We prove that this degree reduces to 5 in the case of the three pairs of isotropic lines of three finite square-pixel cameras. We show that the fifth-degree SLCV has three singularities of multiplicity three, given by the three principal planes of the cameras. This result is used in Algorithm 1 (see Table 2) to generate a bidimensional parameterization of the candidate planes at infinity compatible with three square-pixel cameras. This parameterization, together with the additional data given by another two or more square-pixel cameras permits to identify the true plane at infinity through a two-dimensional optimization process, leading to Algorithm 2 (see Table 3). However, the technique could as well use other additional data such as some scene constraints.

Experiments with real images for the autocalibration of scenes with 5 or more cameras with square pixels and otherwise varying parameters are provided, showing the good performance of the proposed technique compared to other autocalibration methods. In the absence of knowledge about the principal point of the cameras, the SLCV algorithm turns out to be the only feasible approach to solve the autocalibration problem in the minimal case of 5 cameras up to the case of 9 cameras. For 10 or more cameras, the results are similar to those of the AQC algorithm. Table 1 summarizes the similarities and differences between the autocalibration approaches based on the AQC and the SLCV.

The paper is organized as follows: The basic background for the problem is briefly recalled in section 2. Section 3 presents the SLCV along with the basic algebraic geometry

tools required for its definition and analysis as well as our main theoretical results. The algorithms motivated by these results are presented in section 4 and the corresponding experiments are shown in section 5. Conclusions of the paper are found in section 6. An advance of some of the results of this paper appeared in the conference paper [3].

## 2 Camera model, square pixel cameras and projective calibration

We suppose that the cameras can be described using the pin-hole camera model [6], which is defined by the optical center  $\mathbf{C}$  and the projection plane endowed with an affine coordinate system given by the pixel structure of the camera.

The equations of the projection are of the form  $\mathbf{x} \sim \mathbf{P}\mathbf{X}$  where  $\mathbf{P} = \mathbf{K}(\mathbf{R} | -\mathbf{R}\tilde{\mathbf{C}})$ ,  $\mathbf{X} = (X, Y, Z, T)^\top$  are the homogeneous Euclidean coordinates of a 3D point,  $\mathbf{x} = (x, y, z)^\top$  are the homogeneous coordinates of its projection,  $\mathbf{R}$  is a rotation matrix,  $\tilde{\mathbf{C}}$  are the inhomogeneous Euclidean coordinates of the optical center, and  $\mathbf{K}$  is the intrinsic parameter matrix, given by

$$\mathbf{K} = \begin{pmatrix} fm_x & -fm_x \cot \theta & u_0 \\ 0 & fm_y / \sin \theta & v_0 \\ 0 & 0 & 1 \end{pmatrix},$$

where  $f$  is the focal length,  $m_x$  and  $m_y$  are the number of pixels per distance unit in image coordinates in the  $x$  and  $y$  directions,  $\theta$  is the skew angle and  $(u_0, v_0)$  is the principal point.

If the camera aspect ratio  $\tau = m_y/m_x$  and the skew angle  $\theta$  are known, the affine coordinate transformation

$$\mathbf{A} = \begin{pmatrix} \tau \cos \theta & 0 \\ 0 & \sin \theta & 0 \\ 0 & 0 & 1 \end{pmatrix}$$

of the image plane permits to assume that the intrinsic parameter matrix has the form

$$\mathbf{K} = \begin{pmatrix} \alpha & 0 & u'_0 \\ 0 & \alpha & v'_0 \\ 0 & 0 & 1 \end{pmatrix}, \quad (1)$$

which is the intrinsic parameter matrix of a square pixel camera, i.e., one for which  $\tau = 1$  and  $\theta = \pi/2$ .

The back-projected lines of cyclic points at infinity  $\mathbf{I} = (1, i, 0)^\top$  and  $\bar{\mathbf{I}} = (1, -i, 0)^\top$  are the *isotropic lines* of the camera. These lines intersect the absolute conic, for if  $\mathbf{X} = (X, Y, Z, 0)^\top$  is the intersection of one of these two lines with the plane at infinity, we have

$$(1, \pm i, 0)^\top \sim \mathbf{P}\mathbf{X} = \mathbf{K}\mathbf{R}(X, Y, Z)^\top,$$

so that

$$(X, Y, Z)^\top \sim \mathbf{R}^\top \mathbf{K}^{-1} (1, \pm i, 0)^\top,$$

and then

$$\begin{aligned} X^2 + Y^2 + Z^2 &= (X, Y, Z)(X, Y, Z)^\top \\ &= (1, \pm i, 0) \mathbf{K}^{-\top} \mathbf{R} \mathbf{R}^\top \mathbf{K}^{-1} (1, \pm i, 0)^\top \\ &= (1 \pm i) \begin{pmatrix} \alpha^{-2} & 0 \\ 0 & \alpha^{-2} \end{pmatrix} \begin{pmatrix} 1 \\ \pm i \end{pmatrix} = 0. \end{aligned}$$

This equation can be expressed as

$$\mathbf{I}^\top \omega \mathbf{I} = 0, \quad \bar{\mathbf{I}}^\top \omega \bar{\mathbf{I}} = 0, \quad (2)$$

which is the square pixel condition in terms of the image of the absolute conic (IAC)  $\omega = (\mathbf{K}\mathbf{K}^\top)^{-1}$ .

We recall here [6] that it is possible to obtain a projective calibration from image point correspondences only. This means that, given a sufficient number of projected points  $\mathbf{x}_{ij}$  obtained with  $N_c \geq 2$  cameras, we can obtain a set of matrices  $\hat{\mathbf{P}}_i$  and a set of point coordinates  $\hat{\mathbf{X}}_j$  such that  $\mathbf{x}_{ij} \sim \hat{\mathbf{P}}_i \hat{\mathbf{X}}_j$ , where  $\hat{\mathbf{P}}_i = \mathbf{P}_i \mathbf{H}^{-1}$  and  $\hat{\mathbf{X}}_j = \mathbf{H} \mathbf{X}_j$  for some non-singular  $4 \times 4$  matrix  $\mathbf{H}$ .

*Euclidean calibration* can be defined as the obtainment of a matrix  $\mathbf{H}$  changing the projective coordinates of a given projective calibration to some Euclidean coordinate system. It is well-known that Euclidean calibration up to a scale factor is equivalent to the recovery of the absolute conic at infinity  $\Omega_\infty$ .

## 3 The six line conic variety

Let us suppose we have a projective calibration of three square pixel cameras (or, as explained before, cameras with known pixel shape) and let  $\mathbf{P}_i$  be their camera matrices and  $\mathbf{C}_i$  their centers,  $i = 1, 2, 3$ . Let us denote by  $l_i, \bar{l}_i$  the isotropic lines of camera  $i$ . The plane at infinity  $\pi_\infty$  will intersect these lines in points of the absolute conic. Therefore the planes  $\pi$  candidates to be the plane at infinity are those intersecting the isotropic lines in points of a conic (see Figure 1). We are going to see that these planes are given by a 5th-degree algebraic equation in the coordinates  $\pi = (u_1, u_2, u_3, u_4)^\top$  of the plane. In order to obtain this equation, some mathematical preliminaries are needed.

### 3.1 The equation of the six-line conic variety

We recall that lines of  $\mathbb{P}^3$  are in one-to-one correspondence with non-null singular antisymmetric  $4 \times 4$  matrices defined up to a non-zero scalar factor. The correspondence is given by the mapping that assigns to the line  $l$  passing through points  $\mathbf{p}, \mathbf{q}$  the Plücker matrix  $\mathbf{L} = \mathbf{M}(\mathbf{p}, \mathbf{q}) = \mathbf{p}\mathbf{q}^\top - \mathbf{q}\mathbf{p}^\top$  [6]. There is an equivalent mapping attaching to the line determined by planes  $\alpha, \beta$  the matrix  $\mathbf{L}^* = \mathbf{M}(\alpha, \beta)$ . These two

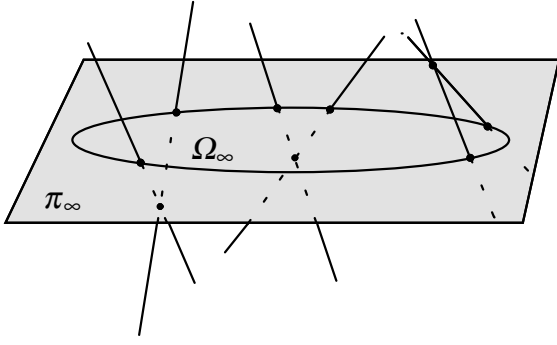


**Fig. 1** Illustration of the incidence relations between the isotropic lines of three cameras, the plane at infinity and the absolute conic.

matrices are related by the transformation  $*$ :  $L = (m_{ij}) \mapsto L^*$  where

$$L^* = \begin{pmatrix} 0 & m_{34} & m_{42} & m_{23} \\ -m_{34} & 0 & m_{14} & m_{31} \\ -m_{42} & -m_{14} & 0 & m_{12} \\ -m_{23} & -m_{31} & -m_{12} & 0 \end{pmatrix}.$$

We also recall that the intersection of the line of Plücker matrix  $L$  with the plane  $\pi = (u_1, u_2, u_3, u_4)^\top$  is the point  $\mathbf{p} = L\pi$ , which is zero if and only if the line  $L$  is contained in  $\pi$ .

If  $H$  is a coordinate change  $\mathbf{X}' = H\mathbf{X}$ , the line  $L$  is written in the new coordinate system as

$$L' = HLH^\top. \quad (3)$$

The degree-two Veronese mapping  $v_2: \mathbb{P}^n \rightarrow \mathbb{P}^N$ ,  $N = n(n+3)/2$ , is defined by

$$v_2(x_1, \dots, x_{n+1})^\top = ((x_i x_j)_{i \leq j})^\top.$$

In particular, for  $n = 2, 3$  we define:

$$\begin{aligned} v_2(x_1, x_2, x_3)^\top &= (x_1^2, x_1 x_2, x_1 x_3, x_2^2, x_2 x_3, x_3^2)^\top, \\ v_2(x_1, x_2, x_3, x_4)^\top &= (x_1^2, x_1 x_2, x_1 x_3, x_1 x_4, x_2^2, \\ &\quad x_2 x_3, x_2 x_4, x_3^2, x_3 x_4, x_4^2)^\top \end{aligned}$$

Observe that a point  $\mathbf{x} \in \mathbb{P}^2$  belongs to the conic of matrix  $C = (c_{ij})$  if and only if

$$v_2(\mathbf{x})^\top \bar{C} = 0, \text{ where } \bar{C} = \left( c_{11}, \frac{c_{12}}{2}, \frac{c_{13}}{2}, c_{22}, \frac{c_{23}}{2}, c_{33} \right)^\top.$$

Therefore the points  $\mathbf{q}_1, \dots, \mathbf{q}_6 \in \mathbb{P}^2$  lie on a conic if and only if

$$\det(v_2(\mathbf{q}_1) \cdots v_2(\mathbf{q}_6)) = 0.$$

Analogously, 10 points  $\mathbf{q}_i$  lie on a quadric of  $\mathbb{P}^3$  if and only if

$$\det(v_2(\mathbf{q}_1), \dots, v_2(\mathbf{q}_{10})) = 0.$$

Next we use the Veronese mapping to characterize whether the intersection of lines with a plane is contained in points of a conic.

**Result 1** Given six lines with Plücker matrices  $L_i$  and vectors  $\pi, \mathbf{a}_1, \dots, \mathbf{a}_4 \in \mathbb{C}^4$ , let us consider the polynomial

$$D(\pi, \mathbf{a}_1, \dots, \mathbf{a}_4) = \det(v_2(L_1\pi), \dots, v_2(L_6\pi), v_2(\mathbf{a}_1), \dots, v_2(\mathbf{a}_4)). \quad (4)$$

The set of planes  $\pi$  intersecting the six lines in points of a conic is defined by

$$D(\pi, \mathbf{a}_1, \dots, \mathbf{a}_4) = 0 \text{ for all } \mathbf{a}_1, \dots, \mathbf{a}_4 \in \mathbb{C}^4.$$

*Proof* First note that if  $D(\pi, \mathbf{a}_1, \dots, \mathbf{a}_4) = 0$ , the points  $L_i\pi, \mathbf{a}_j$  lie on a quadric  $Q$ . By construction, the points  $L_i\pi$  are also on the plane  $\pi$ , and therefore they lie on the conic  $\pi \cap Q$ .

Conversely, let us suppose that the points  $L_i\pi$  lie on a conic  $C$  contained in  $\pi$ . Let us choose coordinates  $(x, y, z, t)$  such that the plane  $\pi$  is given by the equation  $t = 0$ . Let  $C(x, y, z) = t = 0$  be the equations of  $C$ . Any quadric  $Q$  containing  $C$  has an equation of the form

$$\alpha C(x, y, z) + t(ax + by + cz + dt) = 0.$$

Given four points  $\mathbf{a}_j = (x_j, y_j, z_j, t_j)^\top$ , it is always possible to find some quadric  $Q$  through them because the points lead to a linear homogeneous system of four equations in the five unknowns  $a, b, c, d, \alpha$  which always admits at least one non-trivial solution. Since the 10 points  $L_i\pi, \mathbf{a}_j$  lie on  $Q$ , we conclude that  $D(\pi, \mathbf{a}_1, \dots, \mathbf{a}_4) = 0$ .  $\square$

Being each column  $v_2(L_i\pi)$  of degree two in  $\pi$ , the equation  $D(\pi, \mathbf{a}_1, \dots, \mathbf{a}_4) = 0$  is of degree 12 in the coordinates of the plane. Next result shows that we can factor out four trivial linear factors and obtain an 8th-degree polynomial in  $\pi$  which is also shown to be independent of the  $\mathbf{a}_j$ .

**Result 2** The set of planes  $\pi$  intersecting the six lines with Plücker matrices  $L_i$  in points of a conic is given by the 8th-degree polynomial equation

$$F(\pi) = 0 \quad (5)$$

defined by the relationship

$$D(\pi, \mathbf{a}_1, \dots, \mathbf{a}_4) = \det(\mathbf{a}_1, \dots, \mathbf{a}_4) (\pi^\top \mathbf{a}_1) \cdots (\pi^\top \mathbf{a}_4) F(\pi), \quad (6)$$

Furthermore, the polynomial  $F$  does not depend on the variables  $\mathbf{a}_j$ .

*Proof* Any plane  $\pi$  through the point  $\mathbf{a}_1$  is a trivial solution of  $D = 0$ , since the seven points  $L_1\pi, \dots, L_6\pi, \mathbf{a}_1$  would lie on the plane  $\pi$  and therefore the ten points lie on the quadric given by  $\pi$  and the plane formed by points  $\mathbf{a}_2, \mathbf{a}_3, \mathbf{a}_4$ . Consequently, the planes through  $\mathbf{a}_1$  produce a linear factor  $\pi^\top \mathbf{a}_1$  of  $D$  and so do the planes through each of the three remaining points  $\mathbf{a}_j$ .

Let us denote  $A = (\mathbf{a}_1, \dots, \mathbf{a}_4)$ . Next we show that  $\det A$  also divides  $D$ . Since the determinant  $\det A$  is irreducible [1,

p.176] when regarded as a polynomial in the coordinates of the points  $\mathbf{a}_j$ , it is enough to show that  $D$  vanishes whenever  $\det A = 0$ , i.e., when the points  $\mathbf{a}_j$  are contained in some plane  $\pi'$ . In such case, the ten points  $L_i\pi$ ,  $i = 1, \dots, 6$  and  $\mathbf{a}_j$ ,  $j = 1, \dots, 4$ , lie in the degenerate quadric  $\pi \cdot \pi'$  so that  $D$  cancels. We have therefore the required factorization (6).

Let us now show that  $F$  does not depend on the variables  $\mathbf{a}_j$ . The degree of the variables  $\mathbf{a}_j$  on the left hand side of (6) is two because the vectors  $v_2(\mathbf{a}_j)$  are homogeneous quadratic in the entries of  $\mathbf{a}_j$  and each of the  $v_2(\mathbf{a}_j)$  appears only once as a column of the determinant. On the right hand side of (6) we have the factor  $\det A$ , which is homogeneous of degree one in each  $\mathbf{a}_j$ , and the factors  $\pi^\top \mathbf{a}_j$ , which are also homogeneous of degree one. Therefore the remaining factor  $F$  does not depend on the  $\mathbf{a}_j$  since otherwise there would be a mismatch between the degrees of both sides of (6).

Finally, let us check that the equation  $F(\pi) = 0$  characterizes the planes intersecting the six lines in points of a conic. Now that we have proven factorization (6), it is trivial that if  $F(\pi) = 0$  then  $D(\pi, \mathbf{a}_1, \dots, \mathbf{a}_4) = 0$  and, by Result 1,  $\pi$  is a plane intersecting the six lines in points of a conic. Conversely, if  $\pi$  intersects the six lines in points of a conic, the determinant  $D$  vanishes for any  $\mathbf{a}_j$ . In particular, choosing any non-coplanar points  $\mathbf{a}_j \notin \pi$ , so that  $\det A \neq 0 \neq \pi^\top \mathbf{a}_j$ , we conclude that  $F(\pi) = 0$ .  $\square$

The surface of  $\mathbb{P}^3$  given by the planes intersecting the six lines in points of a conic will be called the *six-line conic variety* (SLCV).

### 3.2 The SLCV given by the isotropic lines of three finite square-pixel cameras

In the particular case of three finite square-pixel cameras, the configuration of the isotropic lines, which intersect pairwise in the optical centers  $\mathbf{C}_i$ , allows to further simplify the factorization from Result 2.

**Result 3** *Given a projective reconstruction for three finite cameras, the planes at infinity compatible with the square-pixel property of the cameras are given by the real zeros of a 5th-degree polynomial  $G$  given by the following equation:*

$$F(\pi) = (\pi^\top \mathbf{C}_1)(\pi^\top \mathbf{C}_2)(\pi^\top \mathbf{C}_3)G(\pi). \quad (7)$$

*Proof* We have proved in Result 2 that the set of planes intersecting the lines  $L_i$  in points of a conic is given by the zeroes of an 8th-degree polynomial,  $F(\pi)$ . In the case of six isotropic lines of three square-pixel cameras, there are trivial solutions of the equation  $F(\pi) = 0$  which are of no interest, namely those corresponding to planes passing through any of the optical centers  $\mathbf{C}_i$ ,  $i = 1, 2, 3$ . In fact, any plane through any of the  $\mathbf{C}_i$  intersects the six lines in at most five different points. Since five points always lie on a conic,

all the planes of the three stars of planes through the optical centers are zeros of  $F$ . Moreover, these are not candidate planes at infinity since we are assuming finite cameras. Therefore, we can further factorize the polynomial  $F$  as in equation (7).  $\square$

In the context of camera autocalibration, we will also use the term SLCV for the 5th-degree variety, from which the three trivial linear factors have been removed.

A straightforward application of this result is the direct obtainment of the candidate planes at infinity, when two vanishing points are known, as the real solutions of a fifth-degree polynomial equation in one variable (see [3]).

**Corollary 1** *If two points of the plane at infinity are known, there are at most five candidate planes at infinity which can be found solving the 5th-degree equation in the homogeneous coordinates  $\lambda : \mu$*

$$G(\lambda\alpha + \mu\beta) = 0,$$

where  $\alpha$  and  $\beta$  are any two planes intersecting in the line determined by the two points at infinity.

### 3.3 Singularity of the principal planes

From now on, we suppose as above that the six lines are the isotropic lines of three square-pixel cameras. The following result is the key to find a computationally efficient way to parameterize the set of associated candidate planes. For our configuration of three cameras, we will say that a principal plane is *generic* if it does not contain the projection centers of any of the other two cameras.

**Result 4** *Any generic principal plane is a singularity of multiplicity three of the variety of candidate planes  $G(\pi) = 0$ .*

Result 4 suggests to parameterize the set of candidate planes considering the pencils of planes with base contained in one of the principal planes. We will denote by  $l_i, \bar{l}_i$  the pair of lines through the optical center  $\mathbf{C}_i$  and  $L_i, \bar{L}_i$  their Plücker matrices. The corresponding principal planes will be denoted as  $\pi_i$ ,  $i = 1, 2, 3$ . Let us assume that  $\pi_1$  is a generic principal plane. To each pencil of planes that includes  $\pi_1$  we will associate two candidate planes. To parameterize the pencil, we can consider its element  $\xi$  through  $\mathbf{C}_2$ , so the pencil is given by the planes of the form  $\lambda\pi_1 + \mu\xi$  (see Figure 2).

Result 4 guarantees that the 5th-degree polynomial  $G(\lambda\pi_1 + \mu\xi)$  factorizes as

$$G(\lambda\pi_1 + \mu\xi) = \mu^3 H(\lambda, \mu) \quad (8)$$

where  $H$  is a homogeneous polynomial of degree 2 whose zeroes provide the two candidate planes associated to  $\xi$ . The approach of using a triple point to parameterize a 5-th degree variety is illustrated in Figure 3 for the case of a 2D curve.

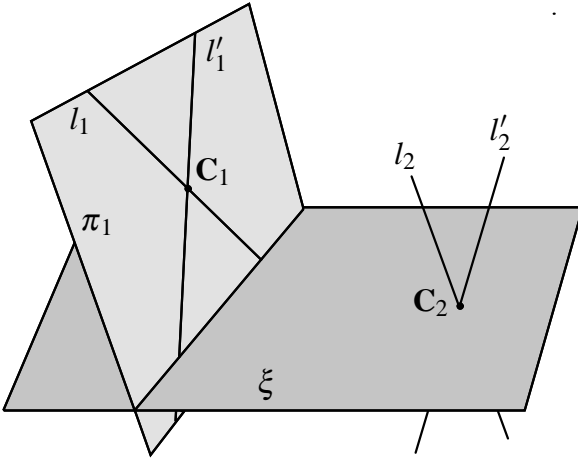


**Fig. 2** Elements in the parameterization of the SLCV given by Result 4.

*Proof* [Proof of Result 4] Using Result 2 we have that

$$\begin{aligned} D &= \det(v_2(L_1\pi), \dots, v_2(\bar{L}_3\pi), v_2(\mathbf{a}_1), \dots, v_2(\mathbf{a}_4)) \\ &= \det(\mathbf{a}_1, \dots, \mathbf{a}_4) (\pi^\top \mathbf{a}_1) \cdots (\pi^\top \mathbf{a}_4) (\pi^\top \mathbf{C}_1) (\pi^\top \mathbf{C}_2) \\ &\quad (\pi^\top \mathbf{C}_3) G(\pi). \end{aligned}$$

With the notation introduced above, let  $\pi = \lambda\pi_1 + \mu\xi$ . Since  $l_1, \bar{l}_1$  are contained in  $\pi_1$  we have  $L_1\pi_1 = \bar{L}_1\pi_1 = \mathbf{0}$  and therefore  $L_1\pi = \mu L_1\xi$  and  $\bar{L}_1\pi = \mu \bar{L}_1\xi$ . Consequently

$$D(\lambda, \mu) = \mu^4 \det(v_2(L_1\xi), v_2(\bar{L}_1\xi), v_2(L_2\pi), \dots, v_2(\mathbf{a}_4)).$$

On the other hand, since  $\mathbf{C}_1 \in \pi_1$ , we have  $\mathbf{C}_1^\top \pi = \mu \mathbf{C}_1^\top \xi$ , so

$$\begin{aligned} &\mu^4 \det(v_2(L_1\xi), v_2(\bar{L}_1\xi), v_2(L_2\pi), \dots, v_2(\mathbf{a}_4)) \\ &= \mu \det(\mathbf{a}_1, \dots, \mathbf{a}_4) (\pi^\top \mathbf{a}_1) \cdots (\pi^\top \mathbf{a}_4) (\xi^\top \mathbf{C}_1) (\pi^\top \mathbf{C}_2) \\ &\quad (\pi^\top \mathbf{C}_3) G(\pi). \end{aligned}$$

Using the genericity of  $\pi_1$  and choosing conveniently the points  $\mathbf{a}_j$  we have that  $\mathbf{C}_2, \mathbf{C}_3, \mathbf{a}_j \notin \pi_1$  for  $j = 1, \dots, 4$ , i.e.,  $\mu$  does not divide any linear factor besides  $\pi^\top \mathbf{C}_1$ . Therefore  $\mu^3$  divides  $G(\lambda\pi_1 + \mu\xi)$  and so  $\pi_1$  is a singular point of  $G$  of multiplicity three.  $\square$

## 4 Algorithms

We have seen that the set of planes compatible with three cameras with square pixels is a surface given by a fifth-degree equation

$$G(\pi) = 0.$$

This will allow to compute the plane at infinity by means of a two-dimensional search if enough additional data about

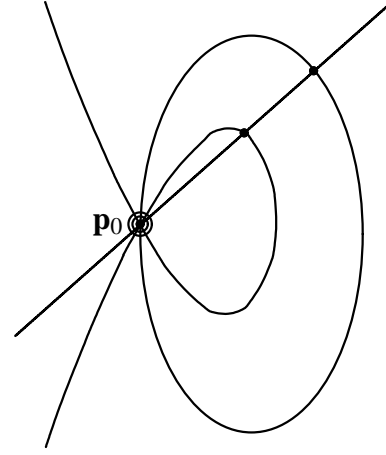


**Fig. 3** Illustration of the approach to obtain the points of the SLCV.

The projective plane curve  $F(\mathbf{p}) = 0$  is of degree five and has  $\mathbf{p}_0$  as a triple point. Therefore, substituting in this equation the parametric equation of a line through this point, results in an equation of the form  $F(\lambda\mathbf{p}_0 + \mu\mathbf{q}_0) = \mu^3 G(\lambda, \mu)$ , so that the other two points of intersection of the line and the curve are obtained by solving the quadratic equation  $G(\lambda, \mu) = 0$ .

The SLCV is a fifth-degree surface in dual space  $\mathbb{P}^{3*}$  and the proposed technique to parameterize is based in computing its intersections with lines through one of its triple points. These lines in  $\mathbb{P}^{3*}$  correspond to pencils of planes in  $\mathbb{P}^3$ .

the cameras or the scene are available. In the first part of this section we will address a convenient way to parameterize the surface of candidate planes, while in the second part we will focus on the particular case in which the additional information stems from the presence of two or more auxiliary square-pixel cameras.

### 4.1 Parameterization of the candidate planes

Exploiting Result 4 and assuming that the first principal plane  $\pi_1$  is generic, our algorithm will sweep the set of candidate planes at infinity corresponding to three square-pixel cameras. We will define a one-to-two mapping attaching to each real line  $l$  of  $\pi_1$  the two candidate planes  $\chi_1, \chi_2$  containing  $l$ , i.e., the intersection of the pencil of planes through  $l$  with the variety of candidate planes. Hence, if we parameterize the set of real lines  $l$  of  $\pi_1$  that do not contain the optical center  $\mathbf{C}_1$ , we will obtain accordingly a two-fold parameterization of the set of candidate planes. To this purpose we fix a point  $\mathbf{r}$  in  $l_1$  which, together with the optical center  $\mathbf{C}_1$  will parameterize the points  $\mathbf{q} \in l_1$  as  $\mathbf{q} = \mathbf{r} + z\mathbf{C}_1$ , being  $z$  a complex number<sup>1</sup>. We now define  $l$  as the line through  $\mathbf{q}$  and  $\bar{\mathbf{q}}$  (see Figure 4).

We will consider as generators of the pencil of planes through  $l$  the principal plane  $\pi_1$  and a plane  $\xi$  passing through

<sup>1</sup> The fixed point  $\mathbf{r}$  may be chosen as the intersection of  $l_1$  with the plane whose coordinates coincide with those of the point  $\mathbf{C}_1$ .

$l$  and  $C_2$ , so the planes of the pencil are of the form

$$\chi = \lambda \pi_1 + \mu \xi.$$

As explained in the previous section, the solutions contained in the pencil through  $l$  will be the zeroes of the polynomial  $H(\lambda, \mu)$  defined in (8). Since it is a homogeneous degree two polynomial, it has an expression of the form

$$H(\lambda, \mu) = A\lambda^2 + B\lambda\mu + C\mu^2, \quad (9)$$

where  $A, B, C$  are polynomials in the coefficients of the Plücker matrices<sup>2</sup>  $L_i, \bar{L}_i$ . Their size, of the order of thousands of terms, is not suitable for algorithmic use. However, a convenient coordinate change shortens them so that they add up to about one hundred terms.

Specifically, denoting by  $\mathbf{q}$  and  $\bar{\mathbf{q}}$  the intersection points of the isotropic lines  $l_1$  and  $\bar{l}_1$  with the plane  $\xi$  and assuming that the points  $C_i, \mathbf{q}$  and  $\bar{\mathbf{q}}$  are in general position, we consider the coordinate change  $H$  performing the mapping

$$\begin{aligned} C_1 &\mapsto (0, 0, 0, 1)^\top \\ C_2 &\mapsto (0, 0, 1, 1)^\top \\ C_3 &\mapsto (0, 1, -1, 1)^\top \\ \mathbf{q} &\mapsto (1, i, 0, 0)^\top \\ \bar{\mathbf{q}} &\mapsto (1, -i, 0, 0)^\top. \end{aligned} \quad (10)$$

In these new coordinates we obtain a polynomial

$$H_0(\lambda, \mu) = A_0\lambda^2 + B_0\lambda\mu + C_0\mu^2, \quad (11)$$

where the coefficients  $A_0, B_0, C_0$  depend only on  $L_2, L_3$ , since  $L_1$  is constant in the new coordinate system.

In Algorithm 1, we assume that the expressions of  $A_0, B_0$  and  $C_0$  have been precomputed (see the appendix for further details).

#### 4.2 Euclidean calibration with five or more cameras

The parameterization provided by the previous Algorithm 1 can be employed, in particular, to perform a two-dimensional search for the plane at infinity using the knowledge provided by two or more additional square-pixel cameras. The next algorithm explores the set of solutions associated to the first three cameras, aiming at the minimization of a cost function

$$C(z) = \min\{C_0(\chi_1(z)), C_0(\chi_2(z))\}, \quad (12)$$

where  $C_0(\chi)$  measures the compatibility of candidate plane  $\chi$  with the square pixel condition of the additional cameras.

For a given  $\chi$ , the IAC of the cameras,  $\omega_i(\chi)$ , is calculated as the conic through the projections of the points of intersection of  $l_i$  and  $\bar{l}_i$ ,  $i = 1, 2, 3$ , with  $\chi$ . Then the cost  $C_0(\chi)$

<sup>2</sup> See appendix B for explicit formulas of Plücker matrices of the isotropic lines.

#### Algorithm 1

##### Objective

Given:

1. a projective calibration of three cameras with optical centers  $C_i$  and isotropic lines  $l_i, \bar{l}_i$  with Plücker matrices  $L_i, \bar{L}_i$ , with generic principal plane  $\pi_1$ ,
  2. a fixed point  $\mathbf{r} \neq C_1$  on the isotropic line  $l_1$  and
  3. a complex number  $z$ ,
- compute the two planes through the points  $\mathbf{q} = \mathbf{r} + zC_1 \in l_1$  and  $\bar{\mathbf{q}} = \bar{\mathbf{r}} + \bar{z}C_1 \in \bar{l}_1$  that intersect isotropic lines  $l_2, \bar{l}_2, l_3, \bar{l}_3$  in points that, together with  $\mathbf{q}$  and  $\bar{\mathbf{q}}$ , lie on a conic.

##### Algorithm

1. With  $\mathbf{q} = \mathbf{r} + zC_1$  compute the matrix of the coordinate change (10) and apply (3) to transform  $L_2$  and  $L_3$ .
2. Using precomputed expressions, calculate the coefficients of the second-degree homogeneous polynomial (11) and its roots  $(\lambda_i, \mu_i)$ ,  $i = 1, 2$ .
3. Obtain the solution planes in the transformed coordinates as  $\chi_i = \lambda_i\pi_1 + \mu_i\xi$ , with  $\pi_1 = (0, 0, 1, 0)^\top$ ,  $\xi = (0, 0, 1, -1)^\top$ ,  $i = 1, 2$  and revert coordinate change for the planes  $\chi_i$ , thus obtaining solution planes  $\chi_1(z), \chi_2(z)$ .

**Table 2** Algorithm to compute two planes  $\chi_1(z), \chi_2(z)$  intersecting the isotropic lines of three square-pixel cameras in points of a conic, where  $z$  parameterizes the set of lines in  $\pi_1$ .

is computed from these IACs. In the course of the algorithm, complex solutions may arise, albeit the actual IAC must be real. Therefore, some additional constraints are taken into account in the design of  $C_0(\chi)$ . In particular, the cost  $C_0(\chi)$  is the maximum of the weighted sum of four non-negative terms:

$$C_0(\chi) = \max_{i=1..N_c} \sum_{k=1}^4 \gamma_k C_k(\omega_i(\chi)), \quad (13)$$

where the weights  $\gamma_k \geq 0$ ,  $C_1(\omega)$  penalizes complex solutions,  $C_2(\omega)$  discourages non positive-definite IACs,  $C_3(\omega)$  measures the square pixel condition (2) and  $C_4(\omega)$  penalizes principal points outside the image domain.

Before computing the individual costs, the IACs  $\omega$  undergo two normalization steps. First, the homogeneous matrix  $\omega$  is scaled by the unit complex number  $s$  that maximizes the Frobenius norm of  $\Re\{s\omega\}$ . This is a constrained optimization problem whose solution is given by a biquadratic equation in  $\Re s$ . Then,  $\omega$  is scaled to unit Frobenius norm,  $\|\cdot\|_F$ .

Next, let us describe each term in (13). If  $\mathbf{u} = \text{vec}(\Re\omega)$  and  $\mathbf{v} = \text{vec}(\Im\omega)$  are the vectorizations of the upper-triangular part of the real and imaginary parts of  $\omega$ ,

$$C_1(\omega) = \|\mathbf{u}\mathbf{v}^\top - \mathbf{v}\mathbf{u}^\top\|_F / (\|\mathbf{u}\|_2^2 + \|\mathbf{v}\|_2^2).$$

The term  $C_2$  is motivated by Sylvester's criterion, which states that a hermitian matrix is positive-definite if and only if all of its leading principal minors are positive. Let  $D_i(A)$ ,  $i =$

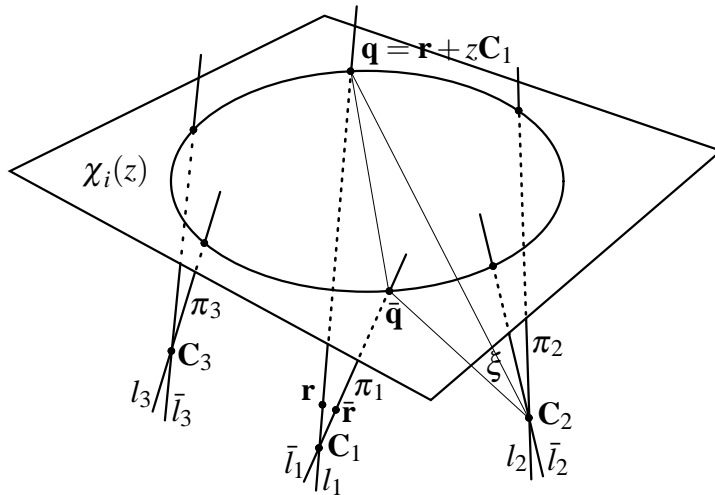


**Fig. 4** Geometric elements used in Algorithm 1. The three square-pixel cameras are represented by their optical centers  $C_j$  and their isotropic lines  $l_j, \bar{l}_j$  contained in the principal planes  $\pi_j$ ,  $j = 1, 2, 3$ . Planes  $\pi_1$  and  $\xi$  are generators of the pencil of planes through the line joining  $\mathbf{q}(z)$  and  $\bar{\mathbf{q}}(z)$ . Within the pencil, solution planes  $\chi_i(z)$ ,  $i = 1, 2$  intersect the six isotropic lines in points of a conic.

1, 2, 3 be the three leading principal minors of matrix  $A$  and  $g(A) = -\sum_{i=1}^3 \min\{0, D_i(A)\}$ , then

$$C_2(\omega) = \min\{g(\Re\{\omega\}), g(\Re\{-\omega\})\},$$

penalizes the non positive-definiteness of the homogeneous matrix  $\omega$ .

The term  $C_3$  measures the deviation from the square pixel condition. We choose:

$$C_3(\omega) = |\tau^2 - 1| + \cos^2 \theta,$$

where  $\tau = m_y/m_x = \omega_{11}/\omega_{22}$  and  $\cos^2 \theta = \omega_{12}^2/(\omega_{11}\omega_{22})$ . Observe that  $C_3(\omega_i) = 0$  for  $i = 1, 2, 3$ , by construction of the SLCV, but not necessarily for the additional cameras. The two terms in  $C_3$  may be weighted differently, too.

The term  $C_4(\omega)$  is the taxicab distance ( $\|\cdot\|_1$ ) from the principal point  $(u_0, v_0)$  to the boundary of the image domain if the principal point lies outside the image domain and zero otherwise. Formulas for  $u_0, v_0$  in terms of  $\omega$  are well known in the literature:  $u_0 = \omega_{13}^*/\omega_{33}^*$  and  $v_0 = \omega_{23}^*/\omega_{33}^*$ , where  $\omega^* \sim \omega^{-1}$ . This term accounts for spurious solutions with unrealistic location of the principal points of the cameras.

Algorithm 2 performs a nonlinear optimization of cost function (12) in two steps. In the first one, the complex plane is sampled and the sample of minimum cost is selected. In the second one, a search for a local minimum is performed using as starting point the complex value provided by the first step.

A sampling of the complex plane that has been empirically found to be useful consists in splitting the plane into the unit disk and its complement, and employing a uniform sampling in modulus and phase for the first, and the inverses of these values for the second. The Nelder-Mead method (downhill simplex method) outperforms other optimization

algorithms with numerical first derivatives such as steepest descent or conjugate gradient.

The Euclidean upgrading may be computed from the stratified approach in Algorithm 10.1 of [6], with the plane at infinity and the IAC of one of the cameras provided by Algorithm 2.

## 5 Experiments

### 5.1 LED bar dataset

The proposed technique has been tested in the calibration of a set of five synchronized square-pixel video cameras with a resolution of  $1280 \times 960$  pixels using a bright point device. Instead of a single-point device, a rigid bar with three light-emitting diodes (LEDs) is employed in the tests. In addition to providing ground truth (the bar length constancy) to test the quality of the results, this allows to use for comparison a calibration algorithm based on the geometry of the captured set of 3D points.

In the experiments, a projective reconstruction of the scene is first obtained for the five cameras. This is accomplished using Algorithm 10.1 of [6] (eight-point algorithm) to compute the fundamental matrix of a pair of cameras and then alternating 12.2 (triangulation) and 7.1 (resection) of [6]. The result is then optimized by projective bundle adjustment [6, p. 434].

Euclidean upgrading is performed using three different techniques: Algorithm 2, an algorithm based on the dual absolute quadric (DAQ), and an algorithm based on the LED bar geometry.

The Euclidean upgrading algorithm based on the DAQ assumes square pixels and principal point at the center of



**Algorithm 2****Objective**

Given a projective calibration of  $N_c \geq 5$  cameras with square pixels, projection matrices  $P_i$  and isotropic lines  $l_i, \bar{l}_i$ , obtain a Euclidean upgrading.

**Algorithm**

1. For each  $z$  in the set  $Z = \{0\} \cup \left\{ \frac{j}{N} e^{i2\pi k/M}, j = 1, \dots, N, k = 1, \dots, M \right\} \cup \left\{ \frac{N-j}{N} e^{-i2\pi k/M}, j = 1, \dots, N-1, k = 1, \dots, M \right\}$ , compute cost  $C(z)$  as follows.
  - (a) Compute planes  $\chi_1(z)$  and  $\chi_2(z)$  using Algorithm 1.
  - (b) For each plane  $\chi \in \{\chi_1(z), \chi_2(z)\}$ ,
    - i. Compute the points of intersection of isotropic lines  $l_i, \bar{l}_i, i = 1, 2, 3$  with the plane, project them with projection matrix  $P_1$  and obtain the matrix  $\omega_1$  of the conic that they define. This is the IAC of the first camera.
    - ii. Obtain the IACs  $\omega_i$  for cameras  $i = 2, \dots, N_c$  by transferring  $\omega_1$  onto them using the plane  $\chi$ ,  $P_1$  and  $P_i$  (Note that the same result would be obtained if the second or third camera was employed). Normalize them to (unit Frobenius norm and maximum real part).
    - iii. Compute  $C_0(\chi)$ , according to equation (13).
  - (c) Compute  $C(z) = \min\{C_0(\chi_1(z)), C_0(\chi_2(z))\}$ .
- Take  $z_0 = \arg \min_{z \in Z} C(z)$ .
2. Perform non-linear optimization to obtain a local minimum  $z_1$  near the value  $z_0$ , repeating steps (a), (b) and (c) above for each evaluation of the function. Choose, of the two planes attached to  $z_1$ , the one with minimum cost  $C_0$ . The Euclidean upgrading is determined by taking this plane at infinity and the associated conic as the absolute conic.

**Table 3** Algorithm to compute a Euclidean upgrading from a projective calibration.

the image. This provides four linear constraints on the DAQ for each camera [21].

The algorithm using the LED bars is based on the fact that three aligned equidistant points determine the point at infinity of the common line [6, p. 50]. Thus each captured position of the LED bar provides a point at infinity in the projective reconstruction, and, therefore, three positions of the bar in the projective reconstruction determine the plane at infinity and, consequently, an affine calibration. Euclidean calibration is then obtained by computing the affinity that makes the lengths of the segments corresponding to captured positions of the rigid bar as close as possible to the true bar length. This requires at least six captures of the bar and the solution of a least-squares problem followed by a Cholesky factorization [20] to determine the affinity up to a Euclidean motion. Affine and Euclidean calibration are repeated 500 times using different random sets of three bars for the affine calibration and all the bars for the Euclidean calibration, and the reconstruction with smallest bar length variance is selected.

After the Euclidean calibration, a Euclidean bundle adjustment is performed, including the enforcement of the square pixel shape and taking into account the lens distortion coefficients (according to the four-parameter OpenCV model [2]).

The sampling parameters in Algorithm 2 have been  $M = N = 50$ , so that the cost function has been evaluated on  $2 \times 50 \times 50 = 5000$  points. Figure 5 shows a sample of the input data for the calibration process. Figure 6 shows two views of the sampled points of the SLCV computed in Algorithm 2. Figure 7 displays the cost function (12) for this experiment, normalized and pseudo-colored from blue (0) to red (1). A logarithmic transformation has been applied to enhance the visualization of small costs. The reconstructed scene obtained with Algorithm 2 is shown in Figure 8. Table 4 shows the reprojection error and the quotient between the standard deviation and the average of the segment lengths for each of the Euclidean upgrading techniques, before and after bundle adjustment.

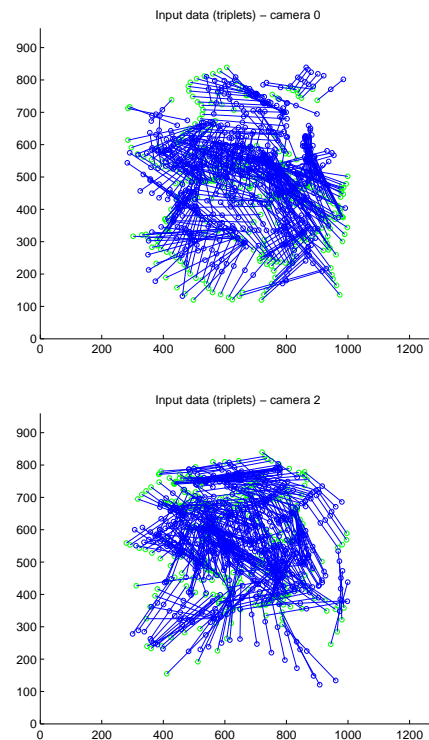


**Fig. 5** Example of input data for the tests (triplets of aligned LEDs in a rigid bar). Only the points are used in the calibration with the proposed algorithms. The triplet structure is used for evaluation purposes.

## 5.2 Checkerboard dataset

The developed method has also been tested on a different set of 5 to 10 images that contain checkerboard patterns [14].

	DAQ		SLCV		Triplets	
	Euc. calib.	Euc. BA	Euc. calib.	Euc. BA	Euc. calib.	Euc. BA
Rep. error	15.04	1.74	1.71	0.64	13.56	0.63
$\sigma/\mu$	0.15	0.029	0.049	0.0098	0.026	0.0048

**Table 4** Results of experiment comparing calibration techniques. The common previous projective calibration shows a reprojection error of 1.23 pixels.  $\sigma$  and  $\mu$  are, respectively, the typical deviation and the average of LED bars lengths.

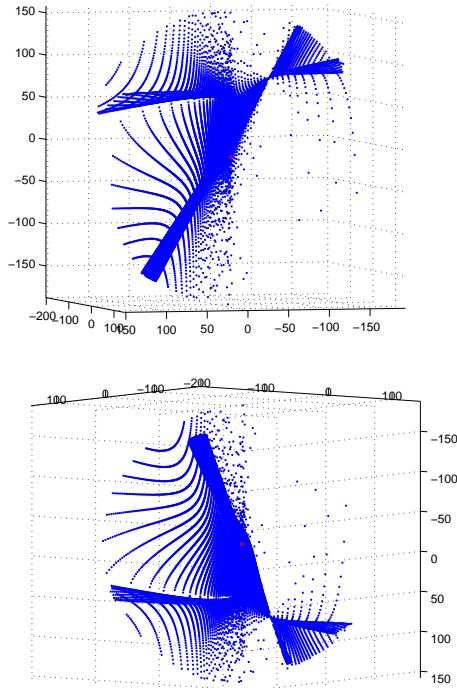


**Fig. 6** Two views of the sampled points of the SLCV.

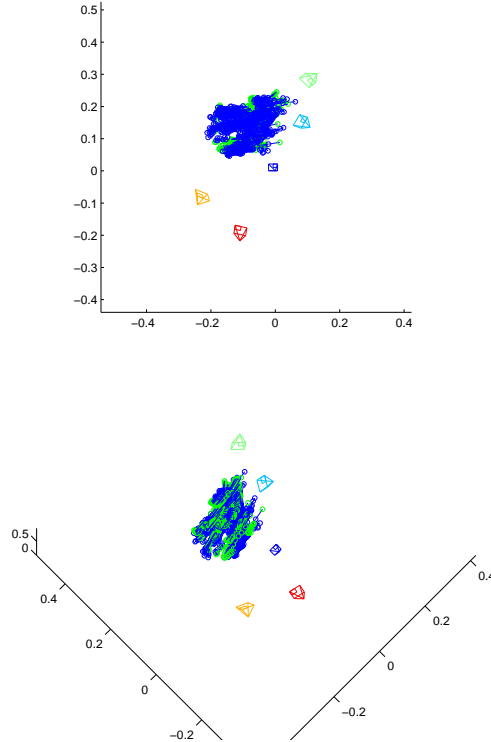


**Fig. 8** Two views of the 3D reconstruction in one of the experiments.

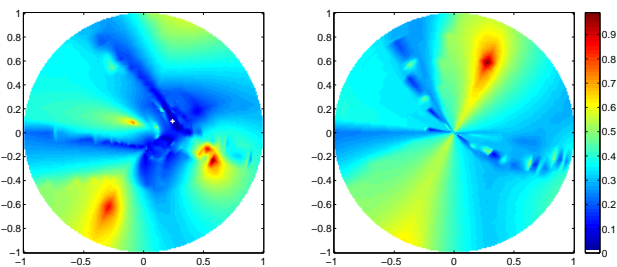


**Fig. 7** Experiment with the LED bar dataset: plots of the sampled cost function. Left: values at the unit disc of the complex plane,  $|z| \leq 1$ . Right: values at the complement of the unit disc, at positions  $1/\bar{z}$ . The white cross in the left plot marks the location of the minimum.

This calibration rig provides an additional validation of the results. The images, of size  $1280 \times 960$  pixels, were acquired with a Sony DSC-F828 digital camera. To test varying parameters, the equivalent focal length (in a 35 mm film) of the camera was set to 50 mm in eight of the images and to 100 mm in the remaining two. Variations due to auto-focus were not controlled. For this range of focal lengths, the lens

distortion (radial and tangential) can be neglected, so it is assumed to be zero.

For each of the following experiments, scale-invariant key points (SIFT [8]) are detected and matched across images, obtained using [17]. Then, a projective reconstruction of the scene is obtained, as already explained. Normalization of coordinates (“preconditioning”) is applied, as it is essential to improve the numerical conditioning of the equations in the different estimation problems involved (fundamental matrix, triangulation, resection and bundle adjustment). Table 5.2 summarizes the parameters of the projective reconstructions. The resulting set of projection matrices are the input to the autocalibration algorithms.

Table 6 shows the results for the experiment with *10 images*. In this case, it is possible to compare the SLCV and DAQ algorithms to a technique based on the AQC [22]. A Euclidean bundle adjustment with enforcement of the square-pixel condition is performed after the Euclidean calibration with each of the four compared techniques. The solution ob-

Method	AQC	DAQ	SLCV	Euc. BA
Mean focal length $\alpha$	1822.9 3433.2	1851.4 3579.3	1806.2 3399.4	1847.8 3555.7
$\alpha$ standard deviation	10.95 36.15	4.86 13.33	16.1 29.21	7.77 4.53
Mean pp $(u_0, v_0)$	(623.1, 463.9) (618.6, 446.8)	(638.1, 477.8) (654.5, 505.7)	(607.4, 468.9) (605.5, 455.4)	(620.4, 485.3) (588.0, 525.2)
p.p. std. dev.	(16.85, 8.13) (34.44, 0.55)	(1.61, 4.96) (17.27, 10.91)	(27.7, 11.15) (53.18, 7.47)	(6.72, 8.71) (24.79, 6.36)
Rep. error	0.65765	0.27181	0.27497	0.22386

**Table 6** Reprojection error and intrinsic parameter comparison for the experiment with 10 images of the Checkerboard scene. For each statistic, the top row corresponds to the value for cameras with  $f = 50$  mm (equivalent in 35 mm film) and the bottom row corresponds to cameras with  $f = 100$  mm. Data are given in pixels.

Scene	Checkerboard		Plaza de la Villa	
# images	10	5	16	5
# 3-D points	1494	1199	8555	1083
# image points	6660	4472	35181	3483
Rep. error (BA)	0.22268	0.17678	0.16053	0.17855

**Table 5** Projective reconstructions.

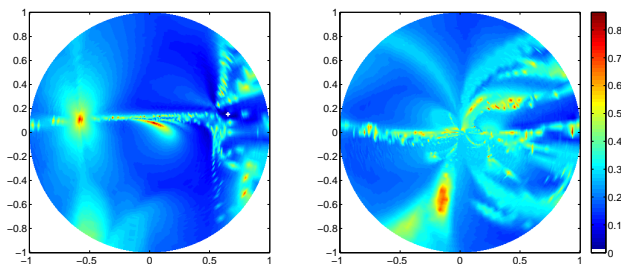


**Fig. 9** Experiment with 10 images of the Checkerboard dataset: plots of the sampled cost function. Left: values at the unit disc of the complex plane,  $|z| \leq 1$ . Right: values at the complement of the unit disc, at positions  $1/\bar{z}$ . The white cross in the left plot marks the location of the minimum.

tained (regardless of the AQC, DAQ or SLCV initialization), is given in the last column of table 6.

If the image resolution and the size of the CCD of the camera are known, it is possible to convert the focal length from mm to pixels. For this dataset, an equivalent focal length of  $f = 50$  mm translates to  $\alpha = 1850$  pixels, which is very close to the values obtained by the different algorithms tested (first row of table 6).

Because the DAQ algorithm yields good estimates of the intrinsic parameters (with small dispersion and reprojection error), we may conclude that the principal point (p.p.) of the camera is close to the center of the image. This observation is also supported by the estimates of the p.p. due to the other algorithms. All three autocalibration methods show a strong agreement with the three-homography calibration algorithm in [14] and [6, p. 211].

Euclidean calibration by means of the developed technique (SLCV) provides competitive results with respect to the other methods (DAQ or AQC), but with a slightly bigger dispersion around the mean values. In normalized coordi-

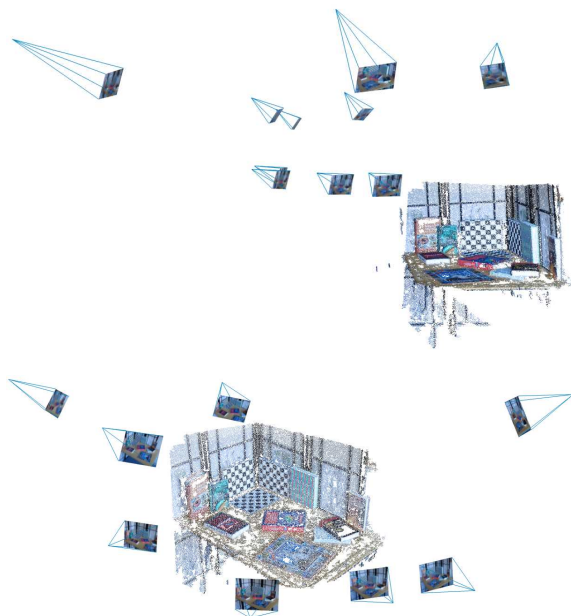


**Fig. 10** Experiment with 10 images of the Checkerboard dataset: reconstructed 3D scene.

nates, the weights used in (13) to measure the goodness of fit of the IACs in Algorithm 2 are  $\gamma_1 = \gamma_2 = \gamma_3 = \gamma_4 = 1$ . The sampling parameters in Algorithm 2 are  $M = N = 100$ . Figure 5.2 shows the sampled cost function. Figure 10 shows two views of the densely reconstructed scene corresponding to the Euclidean calibration by means of the SLCV algorithm. The dense reconstruction was obtained by feeding the images and the Euclidean calibration of the cameras to the Patch-based Multi-view Stereo Software (PMVS) software [5].

Next, an experiment with a subset of 5 images is carried out. To account for varying parameters, three of the images correspond to a focal length  $f = 50$  mm and the remaining two have  $f = 100$  mm. Table 5.2 shows the parameters of the projective reconstruction. Table 7 compares the Euclidean upgrading given by the DAQ and the SLCV algorithms. Both initializations converge to the same solution after Euclidean bundle adjustment (last column of Ta-

Method	DAQ	SLCV	Euc. BA
Mean focal length $\alpha$	1833.3 3511.2	1855.2 3602.1	1883.1 3662.9
$\alpha$ standard deviation	0.46 16.24	3.84 7.90	4.78 26.15
Mean p.p. $(u_0, v_0)$	(637.4, 478.9) (664.2, 493.3)	(624.5, 477.2) (618.0, 492.4)	(620.0, 500.2) (588.8, 569.5)
p.p. std. dev.	(0.72, 2.12) (28.61, 15.91)	(1.41, 1.48) (31.53, 20.03)	(8.72, 0.68) (12.3, 15.4)
Rep. error	0.26204	0.20134	0.17689

**Table 7** Reprojection error and intrinsic parameter comparison for experiment with 5 images of the Checkerboard dataset. Same notation as in Table 6. Both DAQ and SLCV methods yield good results.

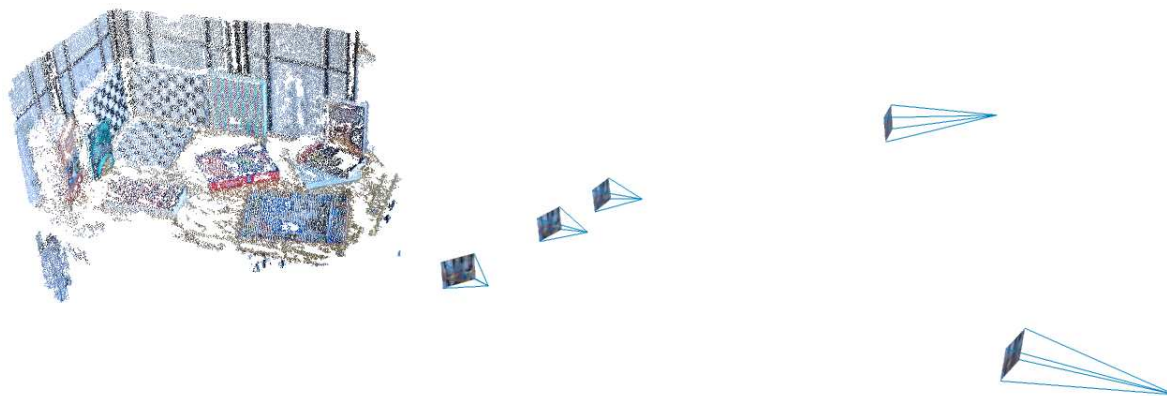


**Fig. 11** Experiment with 5 images of the Checkerboard dataset: reconstructed 3D scene.

ble 7). The SLCV method yields similar results to those of the DAQ method but requiring fewer equations per camera. The reconstructed scene corresponding to the Euclidean calibration by means of the SLCV algorithm is shown in Figure 11. The SLCV method provides a sensible initialization to Euclidean bundle adjustment.

Next, we demonstrate the good performance of the developed method in case of decentered principal point. To do so, the previous 5 images of the Checkerboard dataset are extended to  $1600 \times 1200$  pixels from the upper-left corner. The principal point is, as seen in Table 6, near the point with coordinates  $(640, 480)$  pixels, which significantly differs from the new image center at  $(800, 600)$  pixels. A projective reconstruction of the scene is obtained, with 1197 3-D points, 4463 image projections and a reprojection error of 0.17699 pixels. Table 8 compares the Euclidean upgrading by the two autocalibration methods in Table 7. Because the hypothesis of known principal point (e.g. at the image center) is not satisfied, the DAQ method performs poorly. The SLCV method, however, yields the similar good results as in Table 7 because it solely relies on the square-pixel constraint. The last column of Table 8 shows the result after refining the SLCV Euclidean calibration by bundle adjustment.

### 5.3 Outdoor dataset

As an additional experiment, 16 images of the Plaza de la Villa in Madrid were acquired with an Olympus E-620 digital camera at a resolution of  $1280 \times 960$  pixels. The focal length was set to  $f = 50$  mm ( $\alpha = 1850$  pixels) in half of the images and to  $f = 70$  mm ( $\alpha = 2590$  pixels) in the other half. Reconstructions were carried out with all images and with a subset of 5 images (with different focal lengths). The parameters of the projective reconstructions are summarized in Table 5.2. Figures 12 and 13 show reconstructions of the scene with 16 and 5 images, respectively, obtained by Euclidean upgrading with the SLCV method.

## 6 Conclusions

In this paper we have proposed an algorithm to obtain a Euclidean reconstruction from the minimum possible number of cameras with known pixel shape but otherwise varying parameters, i.e., five cameras. To this purpose we have introduced, as our main tool, the geometric object given by the variety of conics intersecting six given spatial lines simultaneously (the six-line conic variety, SLCV). We have presented an independent and self-contained treatment including a procedure for the explicit computation of the equation of the SLCV defined by three cameras.

Method	DAQ	SLCV	Euc. BA
Mean focal length $\alpha$	3143.7 25499.9	1827.2 3516.0	1877.6 3643.56
$\alpha$ standard deviation	29.28 20080.2	3.87 5.30	5.37 22.69
Mean p.p. $(u_0, v_0)$	(801.3, 516.4) (12192.1, -3639.6)	(622.6, 478.5) (626.0, 493.9)	(617.5, 500.6) (584.0, 571.8)
p.p. std. dev.	(261.1, 44.54) (23167.2, 9700.0)	(6.49, 0.92) (43.46, 7.4)	(7.54, 0.54) (15.97, 9.37)
Rep. error	3324.95	0.20725	0.17707

**Table 8** Reprojection error and intrinsic parameter comparison for experiment with 5 expanded images of the Checkerboard dataset. Same notation as in Table 6. The SLCV method clearly outperforms the DAQ method if the principal point is not near the image center.

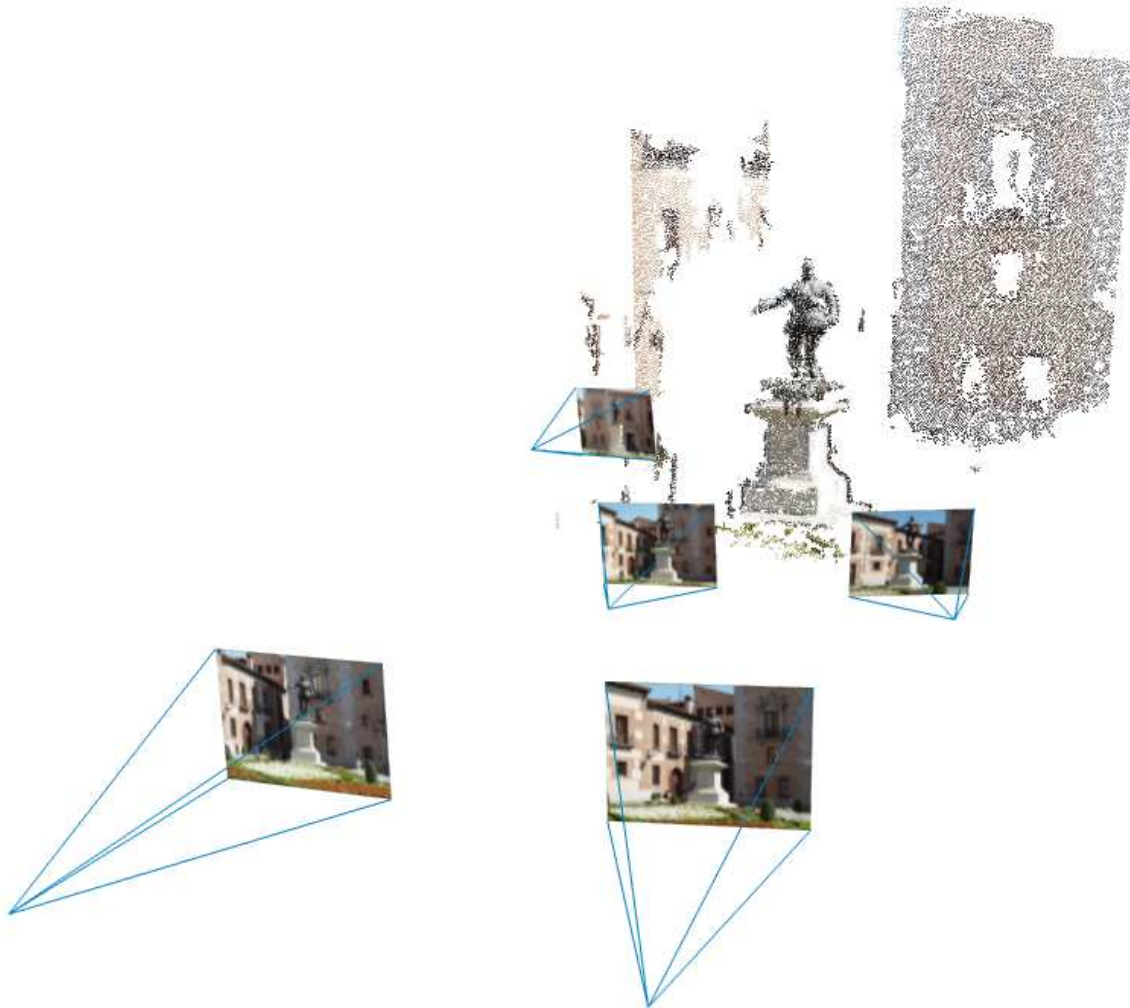


**Fig. 13** Experiment with 5 images of the outdoor dataset: reconstructed 3D scene.

While the SLCV for six lines in generic position is, in general, a surface of degree 8, we have shown that this degree can be reduced to 5 in the case of the three pairs of isotropic lines of three finite square-pixel cameras. We have seen that a direct application of this result is the obtainment of the candidate planes at infinity, when two points at infinity are known.

We have seen that the fifth-degree SLCV has three singularities of multiplicity three. We have used this fact to obtain a computationally efficient parameterization of the SLCV that, if we have some additional data, permits the obtainment of the plane at infinity by means of a two-dimensional search. An algorithm has been proposed for the case in which two or more additional cameras are available.



**Fig. 12** Experiment with 16 images of the outdoor dataset: reconstructed 3D scene.

Experiments with real images for the autocalibration of scenes with 5, 10 and 16 cameras have been given, showing the good performance of the SLCV technique. Particularly, in the case of fewer than 10 cameras, so that the AQC cannot be used, the SLCV method overcomes the limitation of the DAQ based technique for camera autocalibration with varying parameters, i.e., the need for known principal point. Thus, the developed method seems to be the only one that solves the autocalibration problem in the above situation without requiring previous initialization. Furthermore, we have shown that the SLCV method is also a sound alternative to other approaches that require 10 or more cameras or some knowledge of the principal point.

### A Computation of polynomial $H_0$

The polynomial  $H_0(\lambda, \mu) = A_0\lambda^2 + B_0\lambda\mu + C_0\mu^2$  in equation (11) can be computed as follows. Performing the coordinate change (10), the

Plücker matrices of the lines  $l_i$  are

$$\begin{aligned} L_1 &= \mathbf{C}_1 \mathbf{q}^\top - \mathbf{q} \mathbf{C}_1^\top = \begin{pmatrix} 0 & 0 & 0 & -1 \\ 0 & 0 & 0 & -i \\ 0 & 0 & 0 & 0 \\ 1 & i & 0 & 0 \end{pmatrix}, \\ L_2 &= \mathbf{C}_2 \mathbf{p}_2^\top - \mathbf{p}_2 \mathbf{C}_2^\top = \begin{pmatrix} 0 & 0 & -x_2 & -x_2 \\ 0 & 0 & -y_2 & -y_2 \\ x_2 & y_2 & 0 & -z_2 \\ x_2 & y_2 & z_2 & 0 \end{pmatrix}, \\ L_3 &= \mathbf{C}_3 \mathbf{p}_3^\top - \mathbf{p}_3 \mathbf{C}_3^\top = \begin{pmatrix} 0 & -x_3 & x_3 & -x_3 \\ x_3 & 0 & z_3 + y_3 & -y_3 \\ -x_3 & -y_3 - z_3 & 0 & -z_3 \\ x_3 & y_3 & z_3 & 0 \end{pmatrix}, \end{aligned}$$

where the points  $\mathbf{p}_i = (x_i, y_i, z_i, 0)^\top$  are the intersection of lines  $l_i$  with the plane  $\pi_4 = (0, 0, 0, 1)^\top$ . The Plücker matrices  $\bar{L}_i$  are just the complex conjugate of the matrices  $L_i$ . Substituting in equation (4) and factoring out the trivial linear factors we obtain the polynomial  $H_0(\alpha, \beta)$ . Explicit formulas can be found in <http://www.gti.ssr.upm.es/~jir/SLCV.html>.

### B Calculation of the isotropic lines

The isotropic lines are the back-projection of the cyclic points at infinity  $(1, \pm i, 0)^\top$ . Let us see how we can compute their Plücker matrices from the rows of the corresponding projection matrix  $\mathbf{P}$ . In a projective reference in which  $\mathbf{P} = (\mathbf{p}_1, \mathbf{p}_2, \mathbf{p}_3)^\top$ , the back-projection of the cyclic points is given by those  $\mathbf{X} \in \mathbb{P}^3$  such that

$$\mathbf{P}\mathbf{X} \sim (1 \pm i \ 0)^\top.$$

Therefore the cross-product

$$\mathbf{P}\mathbf{X} \times (1 \pm i \ 0)^\top = 0,$$

or, equivalently,  $\mathbf{X}$  satisfies the equations

$$\mathbf{p}_3^\top \mathbf{X} = 0 = (\mathbf{p}_2^\top \pm i \mathbf{p}_1^\top) \mathbf{X}.$$

Hence, the isotropic lines are defined by the intersection of the planes  $\mathbf{p}_3$  and  $\mathbf{p}_2 \pm i \mathbf{p}_1$ . Finally, their Plücker matrices are given by

$$\mathbf{L} = \mathbf{M}(\mathbf{p}_3, \mathbf{p}_2 + i \mathbf{p}_1)^*, \quad \bar{\mathbf{L}} = \mathbf{M}(\mathbf{p}_3, \mathbf{p}_2 - i \mathbf{p}_1)^*$$

where  $\mathbf{M}$  and the  $*$  operator were defined in section 3.1.

### References

1. Bôcher, M.: Introduction to Higher Algebra. Dover Phoenix Editions. Dover Publications (2004)
2. Bradski, G.: The OpenCV Library. Dr. Dobb's Journal of Software Tools (2000)
3. Carballeira, P., Ronda, J.I., Valdés, A.: 3d reconstruction with uncalibrated cameras using the six-line conic variety. In: ICIP, pp. 205–208. IEEE (2008)
4. Faugeras, O.: Stratification of 3-d vision: projective, affine, and metric representations. Journal of the Optical Society of America A **12**, 46,548–4 (1995)

5. Furukawa, Y., Ponce, J.: Accurate, dense, and robust multi-view stereopsis. In: CVPR (2007)
6. Hartley, R., Zisserman, A.: *Multiple View Geometry in Computer Vision*, second edn. Cambridge University Press (2003)
7. Heyden, A., Åström, K.: Euclidean reconstruction from image sequences with varying and unknown focal length and principal point. In: Proc. IEEE Conference on Computer Vision and Pattern Recognition. New York, USA (1997)
8. Lowe, D.: Object recognition from local scale-invariant features. In: ICCV, pp. 1150–1157 (1999)
9. Luong, Q.T., Viéville, T.: Canonical representations for the geometries of multiple projective views. *Comput. Vis. Image Underst.* **64**, 193–229 (1996). DOI 10.1006/cviu.1996.0055. URL <http://portal.acm.org/citation.cfm?id=235090.235091>
10. Ma, Y., Soatto, S., Kosecka, J., Sastry, S.: *An Invitation to 3-D Vision*. Springer (2003)
11. Maybank, S.J., Faugeras, O.D.: A theory of self-calibration of a moving camera. *Int. J. Comput. Vision* **8**(2), 123–151 (1992). DOI <http://dx.doi.org/10.1007/BF00127171>. URL <http://portal.acm.org/citation.cfm?id=144382>
12. Pollefeys, M., Gool, L.V.: A stratified approach to metric self-calibration. In: Proc. of the IEEE Conference on Computer Vision and Pattern Recognition, pp. 407–412 (1997). URL [citeseer.ist.psu.edu/article/pollefeys97stratified.html](http://citeseer.ist.psu.edu/article/pollefeys97stratified.html)
13. Ponce, J., McHenry, K., Papadopoulos, T., Teillaud, M., Triggs, B.: On the absolute quadratic complex and its application to autocalibration. In: Proc. IEEE Conference on Computer Vision and Pattern Recognition, vol. 1, pp. 780–787. Washington, DC, USA (2005). DOI <http://dx.doi.org/10.1109/CVPR.2005.256>
14. Ronda, J.I., Valdés, A., Gallego, G.: Line geometry and camera autocalibration. *J. Math. Imaging Vis.* **32**(2), 193–214 (2008). DOI <http://dx.doi.org/10.1007/s10851-008-0095-0>
15. Schröcker, H.P.: Intersection conics of six straight lines. *Beitr. Algebra Geom* **46**(2), 435–446 (2005)
16. Seo, Y., Heyden, A.: Auto-calibration from the orthogonality constraints. In: Proc. International Conference on Pattern Recognition, vol. 01, pp. 1067–1071. Los Alamitos, CA, USA (2000). DOI <http://doi.ieeecomputersociety.org/10.1109/ICPR.2000.905277>
17. Snavely, N., Seitz, S.M., Szeliski, R.: Modeling the world from internet photo collections. *International Journal of Computer Vision* **80**(2), 189–210 (2008)
18. Sturm, P.: Critical motion sequences for monocular self-calibration and uncalibrated euclidean reconstruction. *Computer Vision and Pattern Recognition, IEEE Computer Society Conference on* **0**, 1100 (1997). DOI <http://doi.ieeecomputersociety.org/10.1109/CVPR.1997.609467>
19. Sturm, P.: Self-calibration of a moving zoom-lens camera by pre-calibration. *Image and Vision Computing* **15**(8), 583–589 (1997). URL <http://perception.inrialpes.fr/Publications/1997/Stu97b>
20. Tresadern, P.A., Reid, I.D.: Camera calibration from human motion. *Image Vision Comput.* **26**(6), 851–862 (2008). DOI <http://dx.doi.org/10.1016/j.imavis.2007.10.001>
21. Triggs, B.: Autocalibration and the absolute quadric. In: Proc. of the IEEE Conference on Computer Vision and Pattern Recognition, pp. 609–614. Puerto Rico, USA (1997). URL <http://perception.inrialpes.fr/Publications/1997/Tri97>
22. Valdés, A., Ronda, J.I., Gallego, G.: Linear camera autocalibration with varying parameters. In: Proc. International Conference on Image Processing, vol. 5, pp. 3395–3398. Singapore (2004)
23. Valdés, A., Ronda, J.I., Gallego, G.: The absolute line quadric and camera autocalibration. *International Journal of Computer Vision* **66**(3), 283–303 (2006)